Computing Phase Equilibria by Parallel Excluded Volume Tempering

Thijs J. H. Vlugt and Burkhard Dünweg

Max Planck Institute for Polymer Research

Ackermannweg 10, D-55128 Mainz, Germany

We present a Monte Carlo scheme for the computation of phase equilibria at high densities. At these high densities, all conventional simulation techniques that rely on insertions and deletions of particles, *e.g.* the Gibbs ensemble technique, will have problems because the acceptance probability for these moves is very low. Furthermore, the efficiency of these methods strongly depends on the complexity of the system, *e.g.* degree of polymerization and branching of the components.

Our new method is based upon simulating a path of independent systems in the grand-canonical ensemble. Each system has a slightly different interaction potential, ranging from a full excluded volume potential to an ideal gas, as well as different imposed chemical potentials of each component. This path is constructed in such a way that the average number of molecules of a specific component per system is constant along the path. To sample all systems of the path efficiently, we apply a parallel tempering procedure to exchange configurations of two adjacent systems. The advantage of these exchanges is that, for the full excluded volume system, one does not have to rely on particle insertions and deletions in this system to sample the full phase space, but rather on particle insertions and deletions in systems with soft interactions. Without excluded volume interactions, the acceptance of insertions is independent of molecular size and shape; hence our method does not suffer from the problems of the conventional methods.

We have tested our method for very simple systems (Lennard-Jones particles) and found exact agreement with Gibbs ensemble simulations. For these simple systems the conventional techniques to compute phase equilibria are much more efficient. However, we expect that for long chain molecules this situation will be reversed.

August 21, 2001

I. INTRODUCTION

There are several numerical techniques to locate phase equilibria of molecular systems[1,2]. One of the most popular techniques, especially suited to locate vapor-liquid equilibria, is the Gibbs Ensemble (GE) technique[3–5]. In this technique, two systems, usually the gas and the liquid phase, are simulated simultaneously in such a way that the systems can exchange both particles and volume. This technique has problems for very dense systems and direct insertion of long chain molecules because particle exchanges between the systems are very unlikely to be accepted and therefore one has problems in sampling the phase space. Unfortunately, for dense systems this is a common feature of both Monte Carlo as well as Molecular Dynamics techniques. A possible way to circumvent the direct insertion of long chain molecules is the use of an expanded grand-canonical ensemble[6,7], which facilitates step-by-step insertion combined with relaxation of the matrix.

For computer simulations of mixtures, it is often very efficient to include trial moves that attempt to change the identity of a molecule. For example, in a GE simulation of small and large particles one could only exchange the small particles between the two systems, as the acceptance probability for particle transfer is much larger for the small particles than for the large ones. Fluctuations in the number of large particles can be sampled by performing a trial move in which a small particle in phase I is transformed into a large particle and simultaneously a large particle in phase II is transformed into a small particle (or vice versa) in such a way that the volumes as well as the reduced particle positions are fixed[8]. Such identity changes only work when the two components do not differ too much in geometry. When the nature of the components is very different, one can use special tricks to perform efficient identity changes. For example, Wijmans *et al.*[9] have developed an algorithm in the GE to exchange a polymer consisting of M monomers with M solvent molecules in the other phase. In this way, one is able to compute thermodynamic properties of a polymer chain in an explicit solvent. Another example is the switch move developed by Martin and Siepmann[10] which combines the identity change in the GE[11] with chain interconversion using Configurational-Bias Monte Carlo[2,12–15], *i.e.* the identity of two chains in two different boxes is changed by passing monomers from one chain to the other. This trial move has also been used by Vlugt *et al.* in the grand-canonical ensemble to study the adsorption of mixtures of linear and branched hydrocarbons in zeolites[16]. However, such methods are not applicable for all systems.

In this paper, we focus on the development of a method to locate phase equilibria that does not depend on particle transfers or identity changes, and therefore does not suffer from these problems. It is important to note that we do not claim that our technique is most efficient for all phase equilibria calculations. Instead, we would like to propose

our method as a general scheme to compute phase equilibria if all other conventional techniques fail.

In our method, we simulate a path of systems in the grand-canonical ensemble. Each system has different imposed chemical potentials as well as a different softness of the interparticle potential in such a way that the limiting systems are the ideal gas and the full interaction potential. By allowing exchanges of configurations between adjacent systems, *i.e.* parallel tempering[17,18], we are able to simulate fluctuations in the number of particles efficiently without having to perform particle insertions for full excluded volume systems at high density. Instead, particle exchanges are very efficient for ultra soft potentials, in particular for the ideal gas.

It is important to note that the systems along the path for which parallel tempering is applied may differ in any arbitrary simulation parameter, *e.g.* temperature, density, imposed chemical potential, or interaction strength. Furthermore, one can apply different parameters for different parts of the system. It is also possible to apply parallel tempering in more than one variable. For example, Yan and de Pablo have computed phase diagrams of polymer blends on a lattice by exchanging configurations of different temperature and by changing the state in the expanded ensemble[19], while Vlugt and Smit have combined parallel tempering with respect to the temperature with umbrella sampling[20]. However, it is not obvious at all which is the best possible parameter to apply the parallel tempering procedure to.

To apply parallel tempering successfully, we have to make sure that the phase space densities of two adjacent systems have enough overlap. In practice, this means that the number of systems that is needed scales with $\sqrt{N}$ in which N is the system size[21,22]. Additionally, for a path of systems in the grand-canonical ensemble, we want to make sure that the total number of molecules as well as the composition do not change too much; this is to ensure that the systems have enough overlap, and to take into account that the total number of particles and the composition tend to relax particularly slowly in the fully interacting system. Therefore, we impose the chemical potentials in such a way that the expectation value of the number of particles for all components is approximately constant along the path.

The main advantage of our method is the following. As the system of the softest potential can be equilibrated extremely fast, independent of the molecular topology of the system, the relaxation time of the full excluded volume potential, determined by the time for a system to diffuse from the ideal gas system to the full excluded volume system, τ, will scale with $K^2 \propto V$ in which K is the number of Hamiltonians and V is the volume[22]. As the minimum size of the system that one has to choose is proportional to the size of a molecule, $R \propto M^{1/2}$ for a random walk of a polymer (in which M is the chain length), the overall relaxation time of the system scales as $\tau \propto M^{3/2}$. For a

more detailed discussion, see Ref.[22]. Other methods to insert or remove chain molecules scale exponentially ($\tau \propto \exp[c \times M]$), like for example, Configurational-Bias Monte Carlo or Recoil Growth[23,24] used in the grand-canonical or Gibbs ensemble, while the expanded GE[19] scales like M^2. Furthermore, the efficiency of these methods depend on the complexity of the molecular architecture[25,26]. Therefore, when M becomes large and the molecular architecture is complicated, our excluded volume tempering approach is expected to become competitive or even superior.

The remainder of this article is organized as follows. In Sec. II, we briefly discuss how to construct a path of systems as well as how to locate the phase equilibrium. In Sec. III, we introduce two simple model systems which we have used to test our method, while in Sec. IV the results of our calculations are presented and compared with conventional GE simulations. This results in our conclusion in Sec. V. In the Appendix we will show a systematic method to optimize the strength of the interaction parameters for a given number of Hamiltonians.

II. SIMULATION TECHNIQUE

In this section, we will discuss our simulation technique to compute phase equilibria. In Subsec. II A, we will describe the way in which we perform our simulations, while in Subsec. II B we describe how to choose a path of Hamiltonians in parameter space. The way to compute phase equilibria from these paths is described in Subsec. II C. We derive our equations for the general case of a sequence of interaction potentials U_i, while not changing the temperature T, or $\beta = 1/(k_B T)$, k_B denoting Boltzmann's constant. Of course, the case of tempering with respect to temperature is implicitly included, since changing the temperature is equivalent to just rescaling the potential, as seen from the Boltzmann factor $\exp(-\beta U)$. A similar comment applies for changing pressure or chemical potential, since these can always be viewed as parameters of an effective Hamiltonian which governs the statistical distribution of states. We will come back to the issue of modifying the potential versus changing the temperature in some more detail in Sec. III.

A. Monte Carlo Procedure

In our computations, we simulate K independent three-dimensional systems of equal volume (V) and temperature (T) in the grand-canonical ensemble. The total partition function of this system equals[2]

$$Q = \prod_{i=1}^{K} Q_i, \tag{1}$$

where Q_i is the grand-canonical partition function for system i. For a binary system, we can write

$$Q_i(\mu_A(i),\mu_B(i),V,T) = \sum_{N_A=0}^{\infty}\sum_{N_B=0}^{\infty} \frac{\exp\left[\beta\left(\mu_A(i)N_A+\mu_B(i)N_B\right)\right]V^{N_A+N_B}}{\Lambda_A^{3N_A}\Lambda_B^{3N_B}N_A!N_B!}\times \int d\mathbf{s}^{N_A}\int d\mathbf{s}^{N_B}\exp\left[-\beta U_i\left(\mathbf{s}^{N_A},\mathbf{s}^{N_B}\right)\right], \tag{2}$$

in which $\mu_A(i)$ and $\mu_B(i)$ are the imposed chemical potentials of components A and B, respectively, while N_A and N_B are the number of particles of components A and B, respectively. For a single-component system, the second sum would have to be restricted to the term $N_B = 0$. Λ_α is the thermal de Broglie wavelength of component α, which, in the framework of strictly classical statistical physics, just serves as a normalization constant to render the partition function dimensionless, and to fix the reference state of the chemical potential. The reduced particle coordinate $\mathbf{s}$ is a three-dimensional vector in the unit cube $[0,1]^3$.

For a binary system, it is convenient to use a "magnetic" language where we transform from N_A and N_B to the total number of particles $N = N_A + N_B$, and the magnetization $M = N_A - N_B$. The corresponding thermodynamically conjugate variables are the total chemical potential $\mu_t = \frac{(\mu_A+\mu_B)}{2}$ and the chemical potential difference $\Delta\mu = \frac{(\mu_A-\mu_B)}{2}$:

$$\mu_A N_A + \mu_B N_B = \mu_t N + \Delta\mu M. \tag{3}$$

For each of the K systems, the interaction strength of the potential, denoted by Γ_i (see Sec. III), differs in such a way that Γ ranges from the ideal gas limit ($\Gamma = 1$, the particles do not interact in any way, and there is no restriction for overlap) to the fully interacting limit ($\Gamma = 0$, both attractive interactions and the excluded volume interaction are fully developed).

In the Monte Carlo (MC) simulation, one first chooses the system i for which a trial move is performed. For the selected system i, we decide at random which trial move is performed:

1. Particle displacement. A particle is chosen at random and given a random displacement from the interval $[-\delta_i,\delta_i]^3$. This trial move is accepted with a probability

$$\mathrm{acc}(o\to n) = \min\left(1,\exp\left[-\beta\Delta U\right]\right), \tag{4}$$

in which ΔU is the energy change. We have used the symbols n and o for the new and old configuration, respectively. The maximum displacement of system i (δ_i) is adjusted such that 35% of all displacements are accepted. In general, one could use any reversible algorithm that simulates an NVT ensemble.

2. Exchange particle with the reservoir. It is decided at random to add or to delete a particle (50% each) and to perform the addition/deletion with component A or B (50% each). The acceptance/rejection rule for these trial moves are[2]

$$\begin{aligned} \mathrm{acc}\left(N_A \to N_A + 1\right) &= \min\left(1, \frac{\Lambda_A^3 \left(N_A + 1\right)}{V} \exp\left[\beta\left(\mu_A - \Delta U\right)\right]\right) \\ \mathrm{acc}\left(N_A \to N_A - 1\right) &= \min\left(1, \frac{V}{\Lambda_A^3 N_A} \exp\left[-\beta\left(\mu_A + \Delta U\right)\right]\right), \end{aligned} \tag{5}$$

and the analogous formulae for component B. It is important to note that the acceptance probability for particle exchanges in system i strongly depends on Γ_i.

3. Exchange of the configuration with system $i+1$ (except for $i = K$):

$$x_i\left(n\right) = x_{i+1}\left(o\right) \quad x_{i+1}\left(n\right) = x_i\left(o\right). \tag{6}$$

To obey detailed balance, this trial move is accepted with a probability[18,19]

$$\mathrm{acc}\left(o \to n\right) = \min\left(1, \frac{w_i\left(x_{i+1}\right) w_{i+1}\left(x_i\right)}{w_i\left(x_i\right) w_{i+1}\left(x_{i+1}\right)}\right), \tag{7}$$

where

$$w_i\left(x_j\right) = \exp\left[-\beta\left(U_i\left(x_j\right) - \mu_t\left(i\right) N\left(x_j\right) - \Delta\mu\left(i\right) M\left(x_j\right)\right)\right]. \tag{8}$$

In this notation, i is referring to the Hamiltonian while j is referring to a set of particle positions. In a typical simulation, we try to choose the difference in softness between adjacent systems in such a way that the fraction of accepted configuration exchanges is around 0.1. In the Appendix, we will show a more systematic approach to choose the soft-core parameters Γ_i.

At this point, it becomes quite evident why, in principle, tempering with respect to temperature is particularly

computationally efficient: In this case, βU_i and βU_{i+1} differ only by a global scaling factor, such that the amount of CPU time required to evaluate the energy change when a system switches Hamiltonians is negligible. This is even more so as the translational degrees of freedom (step 1) require one to calculate energy changes all the time anyways, such that the additional effort of keeping track of the overall energy is also quite small. In contrast, if the Hamiltonian's structure changes between i and $i+1$, then the situation is somewhat different: While for a certain system x_i we do keep track not only of the real energy U_i, but also of the energies U_{i+1} and U_{i-1}, which it would have after a successful switch, we have no information on U_{i+2} or U_{i-2}. One of these latter energies is then needed after a successful switch, and therefore a rejected move is computationally cheaper than an accepted one. For these reasons, a high acceptance rate is not necessarily desirable.

Imposing strict detailed balance does *not* require equality of the probabilities to select a certain system, or type of trial move. However, the probabilities have to be kept fixed during the course of the simulation[2]. In practice, one would like to perform trial moves for systems with strong excluded volume effects more often than for systems without such excluded volume interactions[21]. In our simulations, we typically select the full excluded volume system three times more often than the softest system. In addition, exchanges with the particle reservoir are very unlikely to be accepted for the full excluded volume system, while they are easily accepted in the ideal gas system. Therefore, we only apply particle insertions and deletions to systems that give a reasonable fraction of accepted trial moves. Because of the exchanges of configurations between systems we are still able to have an efficient sampling of the total number of particles and the magnetization of the full excluded volume systems. However, when the number of systems is large the efficiency of sampling fluctuations in composition and total number of particles becomes less efficient.

The reason to perform simulations in the grand-canonical ensemble instead of the canonical ensemble is that we do not have to compute the chemical potentials of each component but rather impose the chemical potentials. This is advantageous because computing the chemical potential of dense systems can be complicated[2]. The price we have to pay for imposing the chemical potential is that we have to compute the first and second moment of both the total number of particles and the magnetization, see Sec. II B.

When a parallel computer is used to do parallel tempering, the naive approach would be to use a homogeneous system decomposition among the processors, which means that every processor is simulating a single system. However, this approach will not be particularly efficient, since there will either be severe synchronization problems (all processors waiting idly until the slowest procedure is finished), or lots of CPU effort wasted due to over-equilibration

of the soft systems (note that these have much smaller correlation times). This effect will be even more pronounced for simulations in the grand-canonical ensemble, for which the acceptance probability for exchanges with the reservoir is essentially zero for most of the systems (except for the system without excluded volume interactions). A better approach would be to simulate more than one system on each processor, in such a way that the number of systems per processor is large for soft systems and small for hard systems. All in all, we feel that our current algorithm, with its quite different treatment of different systems, and, in particular, with its recursive build-up of the tempering path (see Subsec. II B) poses highly non-trivial problems for parallelization, which we consider as far from solved. Therefore, in our current studies, we have only used a single-processor implementation of fairly small systems.

B. Constructing a Path of Systems

When we are simulating a path of K systems, we start for convenience with an ideal gas ($\Gamma = 1$). Therefore, we know immediately how to choose the chemical potentials of components A and B to have a certain average number of particles $(N_A^{(0)}, N_B^{(0)})$:

$$N_\alpha^{(0)} = \frac{V}{\Lambda_\alpha^3} \exp\left[\beta \mu_\alpha\right]. \tag{9}$$

After a certain number of trial moves, we would like to extend the path by one system $(i+1)$. This system has slightly harder interactions than the previous system. For this system $(i+1)$, we impose the chemical potentials in such a way that the ensemble averages of the total number of particles as well as the magnetization is the same as for the previous system (i). In this way, the acceptance probability for configuration exchanges will be reasonably high because there is a large overlap in the number of particles of both components. An estimate for $\mu_t\,(i+1)$ and $\Delta\mu\,(i+1)$ can be obtained by using a Taylor expansion for system i:

$$\begin{aligned} \Delta M = M_{i+1} - M_i \;\approx\; & \left(\Delta\mu\,(i+1) - \Delta\mu\,(i)\right)\left(\frac{\partial\,\langle M\rangle}{\partial \Delta\mu}\right)_i + \\ & \left(\mu_t\,(i+1) - \mu_t\,(i)\right)\left(\frac{\partial\,\langle M\rangle}{\partial \mu_t}\right)_i + \\ & \left(\Gamma\,(i+1) - \Gamma\,(i)\right)\left(\frac{\partial\,\langle M\rangle}{\partial \Gamma}\right)_i \\ = \;& \Delta\Delta\mu\left(\frac{\partial\,\langle M\rangle}{\partial \Delta\mu}\right)_i + \Delta\mu_t\left(\frac{\partial\,\langle M\rangle}{\partial \mu_t}\right)_i + \Delta\Gamma\left(\frac{\partial\,\langle M\rangle}{\partial \Gamma}\right)_i, \end{aligned} \tag{10}$$

$$\begin{aligned}\Delta N = N_{i+1} - N_i \;\approx\; & (\Delta\mu(i+1) - \Delta\mu(i)) \left(\frac{\partial \langle N\rangle}{\partial \Delta\mu}\right)_i + \\ & (\mu_t(i+1) - \mu_t(i)) \left(\frac{\partial \langle N\rangle}{\partial \mu_t}\right)_i + \\ & (\Gamma(i+1) - \Gamma(i)) \left(\frac{\partial \langle N\rangle}{\partial \Gamma}\right)_i \\ =\; & \Delta\Delta\mu \left(\frac{\partial \langle N\rangle}{\partial \Delta\mu}\right)_i + \Delta\mu_t \left(\frac{\partial \langle N\rangle}{\partial \mu_t}\right)_i + \Delta\Gamma \left(\frac{\partial \langle N\rangle}{\partial \Gamma}\right)_i .\end{aligned} \tag{11}$$

We have used the brackets $\langle \cdots \rangle$ to denote an average in the grand-canonical ensemble. The thermodynamic derivatives are estimated from the fluctuation relations

$$\begin{aligned}\frac{\partial \langle M\rangle}{\partial \Delta\mu} &= \beta \left[\langle M^2\rangle - \langle M\rangle^2\right], \\ \frac{\partial \langle M\rangle}{\partial \mu_t} &= \beta \left[\langle MN\rangle - \langle M\rangle \langle N\rangle\right], \\ \frac{\partial \langle M\rangle}{\partial \Gamma} &= -\beta \left[\left\langle M \frac{\partial U}{\partial \Gamma}\right\rangle - \langle M\rangle \left\langle \frac{\partial U}{\partial \Gamma}\right\rangle\right],\end{aligned} \tag{12}$$

$$\begin{aligned}\frac{\partial \langle N\rangle}{\partial \Delta\mu} &= \beta \left[\langle MN\rangle - \langle M\rangle \langle N\rangle\right], \\ \frac{\partial \langle N\rangle}{\partial \mu_t} &= \beta \left[\langle N^2\rangle - \langle N\rangle^2\right], \\ \frac{\partial \langle N\rangle}{\partial \Gamma} &= -\beta \left[\left\langle N \frac{\partial U}{\partial \Gamma}\right\rangle - \langle N\rangle \left\langle \frac{\partial U}{\partial \Gamma}\right\rangle\right].\end{aligned} \tag{13}$$

By computing the fluctuations (equations 12 and 13) for system i, and imposing $\Delta M = \Delta N = 0$, one is able to solve for $\mu_t(i+1)$ and $\Delta\mu(i+1)$ from Eqs. 10 and 11 for a given value of $\Gamma(i+1)$. The value of $\Gamma(i+1)$ should be chosen large enough to reduce the total number of systems (K) but small enough to ensure that configuration exchanges between the systems i and $i+1$ are possible.

After using these equations to generate a first estimate for $\mu_t(i+1)$, $\Delta\mu(i+1)$, one simulates at these values, to (usually) find that $\langle N\rangle$ and $\langle M\rangle$ are not yet equal to the desired values $N^{(0)}$ and $M^{(0)}$. However, one can then use the same set of equations again (this time with $\Delta\Gamma = 0$, and prescribed values of ΔM, ΔN) to iteratively refine the estimates for μ_t and $\Delta\mu$ until satisfactory agreement has been attained. As only first derivatives are used, several iterations are needed.

An important requirement of our method is that the magnitude of the fluctuations in the total number of particles (N) and magnetization (M) of the different systems have enough overlap. As for the sampling of the full excluded

volume system we rely on particle fluctuations in softer systems, the magnitude of these fluctuations in the full excluded volume system should be equal or smaller than those in the softer systems. However, close to the binodal these fluctuations usually increase. When the fluctuations at the binodal are too large, we have to increase the magnitude of the fluctuations at the softer Hamiltonians. A possibility to control the fluctuations in the number of particles is the use of a weight function $W(N,M)$ and performing the individual simulations in the ensemble with partition function π_i:

$$\pi_i = \sum_{N_A=0}^{\infty}\sum_{N_B=0}^{\infty}\frac{\exp\left[W(N,M)+\beta\left(\mu_A(i)N_A+\mu_B(i)N_B\right)\right]V^{N_A+N_B}}{\Lambda_A^{3N_A}\Lambda_B^{3N_B}N_A!N_B!}\times \int d\mathbf{s}^{N_A}\int d\mathbf{s}^{N_B}\exp\left[-\beta U_i\left(\mathbf{s}^{N_A},\mathbf{s}^{N_B}\right)\right]. \tag{14}$$

Ideally, in this ensemble the distributions of M and N should be flat. This requires that

$$W(N,M) = -\ln p(N,M), \tag{15}$$

where $p(N,M)$ is the probability to have a total of N molecules and magnetization M in the original grand-canonical ensemble. The average of a quantity A in the grand-canonical ensemble is recovered by

$$\langle A\rangle = \frac{\langle A\exp\left[-W(N,M)\right]\rangle_\pi}{\langle\exp\left[-W(N,M)\right]\rangle_\pi}. \tag{16}$$

C. Locating the Phase Equilibrium

1. *Phase Equilibrium of a Single Component*

The conditions of equilibrium for two phases containing only one type of particles are that the chemical potential and pressure of the two phases are equal. Imposing equal pressures implies that the grand free energy Ω is equal for both phases[27]:

$$\Omega_i = -p_i V = -\frac{\ln Q_i}{\beta}, \tag{17}$$

provided that the volume of the systems is identical. By differentiating Eq. 2 it is straightforward to show that

$$\left(\frac{\partial\Omega}{\partial\mu}\right)_{T,V,\Gamma} = -\langle N\rangle \tag{18}$$

and

$$\left(\frac{\partial\Omega}{\partial\Gamma}\right)_{T,V,\mu} = \left\langle\frac{\partial U}{\partial\Gamma}\right\rangle, \tag{19}$$

where U is the total energy of the system and N is the number of particles.

The grand free energy of an ideal gas can be derived by integrating Eq. 18 from $\mu = -\infty$ to $\mu = \mu^*$, *i.e.* the chemical potential of the ideal gas at a given density according to Eq. 9. Along that path Eq. 9 of course holds too, such that the ideal gas law results:

$$\Omega\left(\mu^*\right)_{\text{ideal gas}} = -\frac{N\left(\mu^*\right)}{\beta}. \tag{20}$$

Starting from that state, we want to know Ω along the path defined in the previous subsection. Thermodynamic integration, which we perform numerically, yields

$$\Omega = \Omega_{\text{ideal gas}} + \int\left[\frac{\partial\Omega}{\partial\Gamma}d\Gamma + \frac{\partial\Omega}{\partial\mu}d\mu\right], \tag{21}$$

where the integrand is estimated according to Eqs. 18 and 19.

We now wish to find, at fixed Γ, the chemical potential which corresponds to phase equilibrium. Suppose we have data at two (usually, but not necessarily different) chemical potentials μ_I and μ_{II}, where the system simulated at μ_I is in phase I and the data of μ_{II} correspond to phase II. Equating the grand free energies of the two phases up to second order in μ yields

$$\begin{aligned}\Omega_I + \left(\frac{\partial\Omega}{\partial\mu}\right)_I(\mu-\mu_I) + \left(\frac{\partial^2\Omega}{\partial\mu^2}\right)_I\frac{(\mu-\mu_I)^2}{2} = \\ \Omega_{II} + \left(\frac{\partial\Omega}{\partial\mu}\right)_{II}(\mu-\mu_{II}) + \left(\frac{\partial^2\Omega}{\partial\mu^2}\right)_{II}\frac{(\mu-\mu_{II})^2}{2}.\end{aligned} \tag{22}$$

This is a quadratic equation which can be solved for μ easily, since not only the first derivative of Ω is known (Eq.

18), but also the second derivative according to

$$-\frac{\partial^2\Omega}{\partial\mu^2} = \frac{\partial\,\langle N\rangle}{\partial\mu} = \beta\left[\langle N^2\rangle - \langle N\rangle^2\right]. \tag{23}$$

This solution gives a first guess for the coexistence value μ_c. A more precise estimate is found by performing thermodynamic integrations along paths of constant Γ, starting from μ_I and μ_{II}, respectively, into the direction of the solution of Eq. 22. The procedure can be stopped as soon as the solution of the quadratic equation stabilizes. We have also tried to even include the third derivative of Ω, which involves third-moment fluctuations, and to solve the corresponding cubic equation numerically. However, no significant improvement over the second-order approach was found.

2. *General Binary Mixture*

For the gas-liquid transition, the condition $\Omega_I = \Omega_{II}$ uniquely defines a first-order transition line in the two-dimensional parameter space (Γ, μ). For a binary mixture, however, the parameter space $(\Gamma, \mu_t, \Delta\mu)$ is three-dimensional, such that the condition $\Omega_I = \Omega_{II}$ singles out a two-dimensional first-order *sheet*. Usually, however, one is interested in a two-dimensional phase diagram, *i.e.* a one-dimensional cut through the two-dimensional sheet, which depends on the (experimental) conditions and results in a standard first-order line.

The most common experimental condition is that of fixed external pressure p. In the present context, this simply means that we study the phase diagram at a certain fixed value of Ω, which we call $\Omega^{(0)}$. Instead of Eq. 22, we now have the following two equations (here however only up to linear order) to determine μ_t and $\Delta\mu$ at coexistence:

$$\begin{aligned}
\Omega_I + \left(\frac{\partial\Omega}{\partial\mu_t}\right)_I (\mu_t - \mu_{t,I}) + \left(\frac{\partial\Omega}{\partial\Delta\mu}\right)_I (\Delta\mu - \Delta\mu_I) &= \Omega^{(0)}, \\
\Omega_{II} + \left(\frac{\partial\Omega}{\partial\mu_t}\right)_{II} (\mu_t - \mu_{t,II}) + \left(\frac{\partial\Omega}{\partial\Delta\mu}\right)_{II} (\Delta\mu - \Delta\mu_{II}) &= \Omega^{(0)}
\end{aligned} \tag{24}$$

with

$$\begin{aligned}
\left(\frac{\partial\Omega}{\partial\mu_t}\right) &= -\langle N\rangle, \\
\left(\frac{\partial\Omega}{\partial\Delta\mu}\right) &= -\langle M\rangle.
\end{aligned} \tag{25}$$

Of course, this requires to determine Ω_I and Ω_{II} beforehand, which is done via thermodynamic integration, *i.e.* the generalization of Eq. 21 based upon the relations Eqs. 19 and 25. After having found the chemical potentials at coexistence via iterative refinement, one can then determine the properties in both phases. In the most general case, the phases will not only differ in composition, but also in density.

Another possible condition is the situation of having N_A A particles and N_B B particles in a fixed container of volume V. In this case, the two phases will split up into two sub-volumes V_I and V_{II} with $V_I + V_{II} = V$. Introducing $n = N/V$, $m = M/V$, $\Phi = V_I/V$, $n_I = N_I/V$, $m_I = M_I/V$, and the analogous quantities for phase II, we have the conservation laws

$$\begin{aligned} n_I\Phi + n_{II}(1-\Phi) &= n, \\ m_I\Phi + m_{II}(1-\Phi) &= m. \end{aligned} \tag{26}$$

Each of these equations can be solved for Φ; equating the resulting expressions one finds

$$\frac{n - n_{II}}{n_I - n_{II}} = \frac{m - m_{II}}{m_I - m_{II}}. \tag{27}$$

Viewing n_I, n_{II}, m_I, and m_{II} as a function of Γ, μ_t, and $\Delta\mu$, this is the second equation besides $\Omega_I = \Omega_{II}$ which determines the phase equilibrium. We shall not elaborate on this further, since we have only done simulations for the case of a *symmetric* mixture, which is substantially simpler. It should however be noted that the generalization to systems with more than two components is straightforward.

3. *Symmetric Binary Mixture*

For a symmetric mixture, the phase coexistence $\Omega_I = \Omega_{II}$ occurs at $\Delta\mu = 0$. Again, a fixed pressure means a prescribed value of Ω, while in the constant volume ensemble we have $n_I = n_{II} = n$, such that the conservation law for n is satisfied for arbitrary Φ. Conversely, $m_{II} = -m_I$ and hence

$$\Phi = \frac{1}{2}\left(1 + \frac{m}{m_I}\right). \tag{28}$$

Thus, in the symmetric case the conditions for phase coexistence are $\Delta\mu = 0$, and either a prescribed value of Ω (constant pressure), or a prescribed value of N (constant volume).

In our test we have calculated the phase diagram of a symmetric mixture in the constant-volume ensemble. Since we keep N constant along our paths, the phase transition is found by plotting, for a given path, $\Delta\mu$ as a function of Γ and locating the point for which $\Delta\mu = 0$. However, the particle number N is only approximately constant along the path. One therefore again needs an iterative refinement. Starting from an old state (o), we find the refined chemical potential $\mu_t(n)$ of the the new state by requiring

$$\begin{aligned} N(n) &\approx N(o) + (\Delta\mu(n) - \Delta\mu(o)) \left(\frac{\partial N}{\partial \Delta\mu}\right)_o + \\ &\quad (\mu_t(n) - \mu_t(o)) \left(\frac{\partial N}{\partial \mu_t}\right)_o \\ &= N^{(0)} \end{aligned} \tag{29}$$

with $\Delta\mu(n) = 0$, where the thermodynamic derivatives are given by Eq. 13. Again, several iterations are necessary until N has converged. After this, one directly measures M in one of the phases, while, for symmetry reasons, the magnetization in the coexisting phase must be $-M$.

III. MODEL

Quite typically, molecular models are characterized by an interatomic potential $\Phi(r)$ which has both a strongly repulsive core and an attractive tail, the archetype being the well-known Lennard-Jones potential. There may be further potentials involved, *e.g.* to model connectivity, bond bending, torsion, long-range electrostatics, etc., but the basic excluded volume effect is usually taken into account via $\Phi(r)$. Sometimes the attractive part is omitted, if the physics under consideration is not related to attractive interactions. Regardless of these details, however, we may assume, for the phase transitions we are interested in, that the transition is directly related to the properties of $\Phi(r)$. In the case of the gas-liquid transition of a single component, it is necessary that the potential includes an attractive tail; the gas-liquid coexistence then occurs up to the critical temperature T_c, which is, by order of magnitude, given by $k_B T_c = \epsilon$, which is just the depth of the attractive well. For unmixing of two species, attractive interactions are not strictly necessary. Here it is rather the exchange potential $U_{ex} = U_{AA} + U_{BB} - 2U_{AB}$ which matters. Unmixing is expected to occur if U_{ex} is negative at typical interparticle distances; this value of U_{ex} will then, by order of magnitude, determine the critical temperature.

Usually one is interested in the phase diagram in the plane temperature vs. density (or temperature vs. chemical potential) for the gas-liquid transition, and temperature vs. composition (or temperature vs. chemical potential difference) for the unmixing transition. Thus, parallel tempering with respect to temperature has not only the computational advantages outlined above, but also the additional virtue of yielding thermodynamic information one is directly interested in. However, a naive application of temperature tempering would lose the advantage of turning off the excluded volume interaction, since the latter is usually modeled via a singularity in $\Phi(r)$, of which one cannot get rid by simple rescaling. On the other hand, there is no compelling reason to stick to a singularity in $\Phi(r)$. One can rather cut the potential off at some finite value Φ_{max}, which is chosen substantially larger than all temperatures (in units of $k_B T$) where the interesting physics takes place. In that latter temperature regime, which can be estimated beforehand (see above), the behavior of the system will only be minimally altered by this modification. By extending the temperature paths from physically interesting temperatures up to values $k_B T \gg \Phi_{max}$, it is possible to reach the ideal gas limit, which is essential for our approach to work.

The cutoff at Φ_{max} should be rather sharp, for the following reasons: On the one hand, $\Phi(r)$ should be kept as the original potential up to $\Phi = \Phi_{max}$, in order to leave the physics at low temperatures unchanged. On the other hand, potential values substantially larger than Φ_{max} should be avoided, in order to reach the ideal gas limit as quickly as possible. Such a sharp cutoff involves a rather large (perhaps infinite) curvature of Φ, which would cause problems for Molecular Dynamics (MD) or Stochastic Dynamics (SD) algorithms. It is therefore advisable to not try to equilibrate the translational degrees of freedom by MD or SD, but rather by MC, which is unaffected by such problems.

In spite of all these considerations, which seem rather compelling to us if phase diagram calculations of real systems are desired, we have not taken the outlined route in our first simulations. Rather, we simply wanted to perform a feasibility study of the approach as such, and for this purpose to make contact with previous simulations which had been performed in our group. Bunker and Dünweg[22] studied the effect of excluded volume tempering on the equilibration of bead-spring polymer melts, using a modified WCA interaction[28] of the form

$$U(r) = \begin{cases} A - Br^2 & r \le r_t \\ 1 + 4\left[\left(\frac{1}{r}\right)^{12} - \left(\frac{1}{r}\right)^{6}\right] & r_t \le r \le r_c \\ 0 & r_c \le r \end{cases} \tag{30}$$

where the unit system is given by setting both the Lennard-Jones length σ and the Lennard-Jones energy ϵ to unity.

The cutoff is chosen as $r_c = 2^{1/6}$, such that the potential is purely repulsive, while r_t (the "transfer" value) is varied to turn the interaction off. Introducing $\Gamma = r_t/r_c$, one sees that full repulsion occurs for $\Gamma = 0$, while $\Gamma = 1$ corresponds to the ideal gas. The parameters A and B are chosen such that both U and its first derivative are continuous.

Soddemann[29] studied binary A-B mixtures (both simple mixtures and amphiphilic systems) using a purely repulsive WCA interaction (*i.e.* Eq. 30 for $\Gamma = 0$) for unlike species, while A-A and B-B contacts are also subject to an attractive tail:

$$U(r) = \begin{cases} -\phi + 1 + 4\left[\left(\frac{1}{r}\right)^{12} - \left(\frac{1}{r}\right)^{6}\right] & r \le r_c \\ \frac{1}{2}\phi\left[\cos\left(\alpha r^2 + \gamma\right) - 1\right] & r_c \le r \le r_m \\ 0 & r_m \le r \end{cases} \tag{31}$$

where r_c is defined as before, $r_m = 1.5$, and the parameters α and γ are chosen such that the potential and its first derivative are continuous at r_c and r_m, *i.e.* $\alpha r_c^2 + \gamma = \pi$, $\alpha r_m^2 + \gamma = 2\pi$. In Ref.[29] the depth of the potential well, ϕ, was varied in order to drive the unmixing transition. To simulate an asymmetric binary system using such a potential, one could use different values of ϕ for the AA and BB interactions.

Combining these two potentials, we use for studying a binary liquid the potential Eq. 30 for unlike species, while for A-A and B-B contacts we use a modified form of Eq. 31

$$U(r) = \begin{cases} A - Br^2 & r \le r_t \\ -\phi(1-\Gamma) + 1 + 4\left[\left(\frac{1}{r}\right)^{12} - \left(\frac{1}{r}\right)^{6}\right] & r_t \le r \le r_c \\ \frac{1}{2}\phi(1-\Gamma)\left[\cos\left(\alpha r^2 + \gamma\right) - 1\right] & r_c \le r \le r_m \\ 0 & r_m \le r \end{cases} \tag{32}$$

Here the symbols have the same meaning as above. We have studied this system at temperature $k_B T = 1$ and density $\rho = 0.85$ for the single value $\phi = 1$. According to Ref.[29], this is deeply in the unmixed state. Since this system is also an ideal gas for $\Gamma = 1$, *i.e.*, in particular, in the mixed state, we can study the unmixing transition just driven by varying Γ. The results of this calculation will be presented in Sec. IV.

For the gas-liquid transition of a single component, we rather use a modified standard Lennard-Jones potential:

$$U(r) = \begin{cases} A - Br^2 & r \leq r_t \\ 4[1-\Gamma]\left[\left(\frac{1}{r}\right)^{12} - \left(\frac{1}{r}\right)^{6}\right] & r_t \leq r \leq r_{cut} \\ 0 & r > r_{cut} \end{cases} \tag{33}$$

with the usual meaning of symbols and $r_{cut} = 2.5$. We study the gas-liquid transition at $k_B T = 2/3$ as a function of Γ, while the density is varied.

In Fig. 1 (left), we have plotted the potential Eq. 32 for various values of Γ. In the same figure (right), we have plotted the radial distribution function $g(r)$ of the single component system in the NVT ensemble at $\rho = 0.85$, also for various values of Γ. This figure clearly shows the transition from an ideal gas to a liquid. For $\Gamma = 0$, the particles cannot pass each other, while for larger values they can. Interestingly enough, there is a maximum of $g(r)$ at $r = 0$ for intermediate values of Γ. We believe that the origin of this behavior are local clusters of particles. A particle which sits on top of the central particle of the cluster is preferentially located right at the center. Although this maximizes the interaction energy with the central particle, this configuration is particularly stable with respect to the attractive interactions with the surrounding neighbor shell. Apparently the latter dominates in a certain region of Γ values.

IV. RESULTS AND DISCUSSION

In all our simulations, we have used around 10^6 simulation cycles. In a cycle, the number of trial moves equals the number of particles times the number of Hamiltonians. This makes the conventional GE simulations more than an order of magnitude faster. In our GE simulations of mixtures, we have used identity changes to speed up our computations. It is important to note that in GE simulations of symmetric mixtures it is not necessary to perform volume changes or particle exchanges between the boxes[2].

A. Symmetric Binary Mixture

In Fig. 2, we have plotted the phase diagram for a symmetric binary mixture calculated by our parallel tempering method, as well as the result from GE simulations of various system sizes, in the (ρ, Γ) plane. The reasons to choose this plane have been discussed in Sec. III. Here, ρ is the density of one species (number of A particles per unit volume), while the total density is $\rho_t = 0.85$ and the temperature $k_B T = 1$.

In our parallel tempering simulations, we have used 25 different Hamiltonians and an average of $\langle N \rangle = 100$ particles. For a system with $\langle N \rangle = 300$ and 35 Hamiltonians we found exactly the same coexistence densities; the error in the coexistence density is smaller than the symbol size. Clearly, the parallel tempering method gives the same results as the GE method. However, for this system the conventional Gibbs ensemble technique is two orders of magnitude faster that our parallel tempering technique.

In Fig. 3, we have plotted the chemical potentials as well as the quantity $\langle \partial U / \partial \Gamma \rangle$ as a function of Γ for the computation of the phase equilibrium at $\Gamma = 0.55$. Apparently, starting from the ideal gas case, we have to increase the chemical potential to overcome the repulsion until at $\Gamma \approx 0.9$ the attractive part of the potential becomes dominant and therefore the total chemical potential decreases with decreasing Γ. Note that the chemical potential difference, $\Delta\mu$, is almost a linear function of Γ. This can provide us with an initial estimate of the phase coexistence.

In Fig. 4, we have plotted the standard deviation of the number of particles of both components as a function of the Hamiltonian index. When the system approaches the binodal curve, the fluctuations increase slightly; for the systems studied here we still have enough overlap between the distributions to have an adequate sampling. Therefore, in this case we do not need a weight function to enhance fluctuations in the number of particles (Eq. 14).

An important quantity is the distribution of the magnetization M at phase coexistence. This distribution should be identical to the distribution of M obtained in the semi-grand ensemble[2]. However, the (correct) two-peak structure of the distribution is only reproduced in the second case. The reason is that the semi-grand ensemble is able to "flip" the overall system from the A-rich to the B-rich phase, and the two-peak distribution is the result of averaging over a long run in which many of these events have occurred. Conversely, our method samples composition fluctuations only by insertions and deletions in the soft limit, where the system is (uniquely) A-rich. Therefore, B-rich configurations are extremely strongly suppressed, with a statistical weight $\exp(-\text{const.} \times V)$, where V is the system volume. They actually have never been observed during our runs. Effectively, our simulation therefore only samples the A-rich peak of the distribution, see Fig. 5. From the point of view of Markov chains, our method thus suffers, strictly spoken, from ergodicity problems. However, we are only interested in the behavior in the thermodynamic limit, where exactly the same type of non-ergodicity occurs. We hence do not view this feature of the algorithm as a drawback, but rather as an advantage.

B. Single Component System

In Fig. 6 we have plotted the phase diagram for a Lennard-Jones system at $\beta = 1.5$. Again, we find the same results for the coexistence density as for the Gibbs ensemble simulations, except for some small finite size effect near the critical point. The method is thus demonstrated to work for a gas-liquid transition, too. Again, for our simple system the standard GE approach is much more efficient.

V. CONCLUSION

In summary, we have presented a new Monte Carlo technique to compute phase equilibria that does not rely on insertions and deletions of molecules in systems with strong excluded volume interactions. Therefore, our method does not depend on the complexity of the individual molecules. One should expect that this approach, or related variants, might be useful for systems where insertions are particularly difficult, *e.g.* for mixtures whose constituents are complex macromolecules. In particular, we expect the method might outperform conventional approaches if the molecular architecture is non-linear, and even piece-by-piece insertions run into problems.

VI. ACKNOWLEDGMENTS

This work was supported by the EU TMR network "NEWRUP", contract No. ERB-FMRX-CT98-0176. We would like to thank Ralf Everaers, Cameron Abrams, and Alex Bunker for stimulating discussions.

Appendix: How to Choose the Soft-Core Parameters Γ_i

As is explained in the main text of this article, in parallel tempering simulations it is important to choose the Hamiltonians of the individual systems (denoted by the soft-core parameters Γ_i) in such a way that two neighboring systems have enough overlap. This can be done by choosing a large number of Hamiltonians (K). However, this is undesirable because the time that it takes for a single system to diffuse along a path of Hamiltonians is proportional to K^2. Therefore, one has to make a compromise. It is important to note that the number of systems is also constrained by our thermodynamic integration (Eq. 21). Once the number of systems has been chosen, we still have to choose the individual values of Γ_i in such a way that the acceptance rate for exchange moves between two neighboring systems is as uniform as possible. When, for example, the acceptance probability between one pair of systems is

extremely low, then this "bottleneck" is going to influence the overall time that it takes for one system to diffuse from the full excluded volume Hamiltonian to the ideal gas Hamiltonian. The exact same problem is present when the temperature is used as a tempering variable.

A naive way to choose Γ_i would be to do a series of simulations in which the acceptance rate is computed; by comparing a series of simulations we can get a feeling which distribution of Γ is optimal. However, when the number of systems is large this approach will require many simulations. Moreover, by changing a single value of Γ_i the acceptance probabilities of adjacent exchanges will also be influenced. Therefore, such an approach will hardly ever work in practice.

A more systematic, albeit still somewhat heuristic, approach to choose Γ_i would be the following. Suppose that we have K Hamiltonians with soft-core parameters Γ_i in such a way that the endpoints are fixed, for example, $\Gamma_1 = 1$ and $\Gamma_K = 0$. We define a function $A(\Gamma)$ in the following way:

$$p(i, i+1) = \max\left[0, 1 - A\left(\frac{\Gamma_{i+1} + \Gamma_i}{2}\right)|\Gamma_{i+1} - \Gamma_i|\right], \tag{34}$$

in which $p(i, i+1)$ is the acceptance probability of exchanges between system i and $i+1$. Essentially, the acceptance probability increases when Γ_i and Γ_{i+1} are closer; the function $A(\Gamma)$ is describing the sensitivity of the acceptance ratio to the distance between systems $i+1$ and i. In our previous study we found that this sensitivity can be quite big[22]. By performing a short simulation for a given set of Γ, one is able to compute $A(\Gamma)$. We then start a Monte Carlo simulation in which we randomly select a system i and try to change Γ_i. Instead of performing a simulation with the physical system, the new acceptance probabilities are computed using Eq. 34 and using a linear interpolation scheme to compute $A(\Gamma)$. The figure of merit is chosen in such a way that the acceptance rate is as uniform as possible, *i.e.* $\mathcal{H} = \left\langle p(i, i+1)^2 \right\rangle - \langle p(i, i+1) \rangle^2$. Furthermore, we apply the restriction that the soft-core parameters cannot pass each other.

To demonstrate this procedure, in Fig. 7 (left) we have plotted the soft-core parameter Γ_i as a function of the Hamiltonian index i for a typical system in which the acceptance rate is and is not constant. In the right figure, the corresponding acceptance probability of exchanges between systems i and $i+1$ are plotted. Clearly, the fraction of accepted exchange trial moves is very sensitive to Γ_i, which requires a self-consistent method to choose the soft-core parameters.

[1] M.P. Allen and D.J. Tildesley, *Computer Simulation of Liquids* (Clarendon Press, Oxford, 1987).

[2] D. Frenkel and B. Smit, *Understanding Molecular Simulations: from Algorithms to Applications* (Academic Press, San Diego, 1996).

[3] A.Z. Panagiotopoulos, Mol. Phys. **61**, 813 (1987).

[4] A.Z. Panagiotopoulos, Mol. Phys. **62**, 701 (1987).

[5] A.Z. Panagiotopoulos, Mol. Sim. **9**, 1 (1992).

[6] F.A. Escobedo and J.J. de Pablo, J. Chem. Phys. **103**, 2703 (1995).

[7] F.A. Escobedo and J.J. de Pablo, J. Chem. Phys. **105**, 4391 (1996).

[8] A.Z. Panagiotopoulos, N. Quirke, M. Stapleton, and D.J. Tildesley, Mol. Phys. **63**, 527 (1988).

[9] C.M. Wijmans, B. Smit, and R.D. Groot, J. Chem. Phys. **114**, 7644 (2001).

[10] M.G. Martin and J.I. Siepmann, J. Am. Chem. Soc. **119**, 8921 (1997).

[11] J.J. de Pablo and J.M. Prausnitz, Fluid Phase Equilibria **53**, 177 (1989).

[12] J.I. Siepmann and D. Frenkel, Mol. Phys. **75**, 59 (1992).

[13] J.I. Siepmann and I.R. McDonald, Mol. Phys. **75**, 255 (1992).

[14] D. Frenkel, G.C.A.M. Mooij, and B. Smit, J. Phys.: Condens. Matter **4**, 3053 (1992).

[15] J.J. de Pablo, M. Laso, and U.W. Suter, J. Chem. Phys. **96**, 6157 (1992).

[16] T.J.H. Vlugt, R. Krishna, and B. Smit, J. Phys. Chem. B **103**, 1102 (1999).

[17] C.J. Geyer and E.A. Thompson, J. Am. Stat. Assoc. **90**, 909 (1995).

[18] Q.L. Yan and J.J. de Pablo, J. Chem. Phys. **111**, 9509 (1999).

[19] Q.L. Yan and J.J. de Pablo, J. Chem. Phys. **113**, 1276 (2000).

[20] T.J.H. Vlugt and B. Smit, Phys. Chem. Comm. **2**, 1 (2001).

[21] M. Falcioni and M.W. Deem, J. Chem. Phys. **110**, 1754 (1999).

[22] A. Bunker and B. Dünweg, Phys. Rev. E **63**, 16701 (2001).

[23] S. Consta, N.B. Wilding, D. Frenkel, and Z. Alexandrowicz, J. Chem. Phys. **110**, 3220 (1999).

[24] S. Consta, T.J.H. Vlugt, J. Wichers Hoeth, B. Smit, and D. Frenkel, Mol. Phys. **97**, 1243 (1999).

[25] M.G. Martin and J.I. Siepmann, J. Phys. Chem. B **103**, 4508 (1999).

[26] C.D. Wick and J.I. Siepmann, Macromolecules **33**, 7207 (2000).

[27] B.K. Peterson and K.E. Gubbins, Mol. Phys. **62**, 215 (1987).

[28] J.D. Weeks, D. Chandler, and H.C. Andersen, J. Chem. Phys. **54**, 5237 (1971).

[29] T. Soddemann, Ph.D. thesis, University of Mainz, Germany, 2000.

Figure captions

- Figure 1. Left: Potential energy function for various values of the interaction strength Γ (Eq. 32). Right: Radial distribution function for a single component system at $\rho = 0.85$ simulated in the NVT ensemble.

- Figure 2. Phase diagram of a symmetric binary mixture at a total density of $\rho_t = 0.85$ for various system sizes (N). $\beta = 1$. As the mixture is symmetric, the concentration of the other component equals $\rho_b = \rho_t - \rho_A$. The lines show the results from GE simulations, while the symbols represent the results from our parallel tempering algorithm.

- Figure 3. Left: $\Delta\mu$ and μ_t as a function of the interaction strength for the computation of the phase equilibrium at $\Gamma = 0.55$ and $\beta = 1$ for a symmetric binary mixture. Right: $\langle dU/d\Gamma \rangle$ for the same system.

- Figure 4. Standard deviation of the total number of particles of both components as a function of the Hamiltonian index i; $i = 1$ represents the ideal gas ($\Gamma_1 = 1$), $i = 20$ represents the point of the binodal for which the phase equilibrium is computed (here, $\Gamma_{20} = 0.65$). $\langle N \rangle = 106.25$, $\langle M \rangle \approx 90$. The standard deviation σ of component j is defined as $\sigma^2 = \langle N_j^2 \rangle - \langle N_j \rangle^2$ in which N_j is the total number of particles of component j.

- Figure 5. Distribution of the magnetization at $\Gamma = 0.55$ and $\beta = 1$ for a symmetric binary mixture at phase equilibrium ($\Delta\mu = 0$); $\langle N \rangle = 106.25$. This distribution is identical to the distribution obtained from a single semi-grand ensemble simulation with $N = 106$ and $\Delta\mu = 0$ (left figure), except for the region between the two stable states (right figure), and for the fact that we observe only one peak of the distribution, as explained in the text.

- Figure 6. Phase diagram of the Lennard-Jones fluid (Eq. 33); densities as a function of the interaction strength Γ at $\beta = 1.5$. Comparison of our method with standard Gibbs ensemble simulations. Only close to the critical point, there is a small finite size effect.

- Figure 7. Left: Soft-core parameter Γ_i for the optimized (squares) and unoptimized (circles) systems as a function of the Hamiltonian index (i). Right: The average acceptance probability for exchanges between system i and $i + 1$.

Figure 1 (Left)

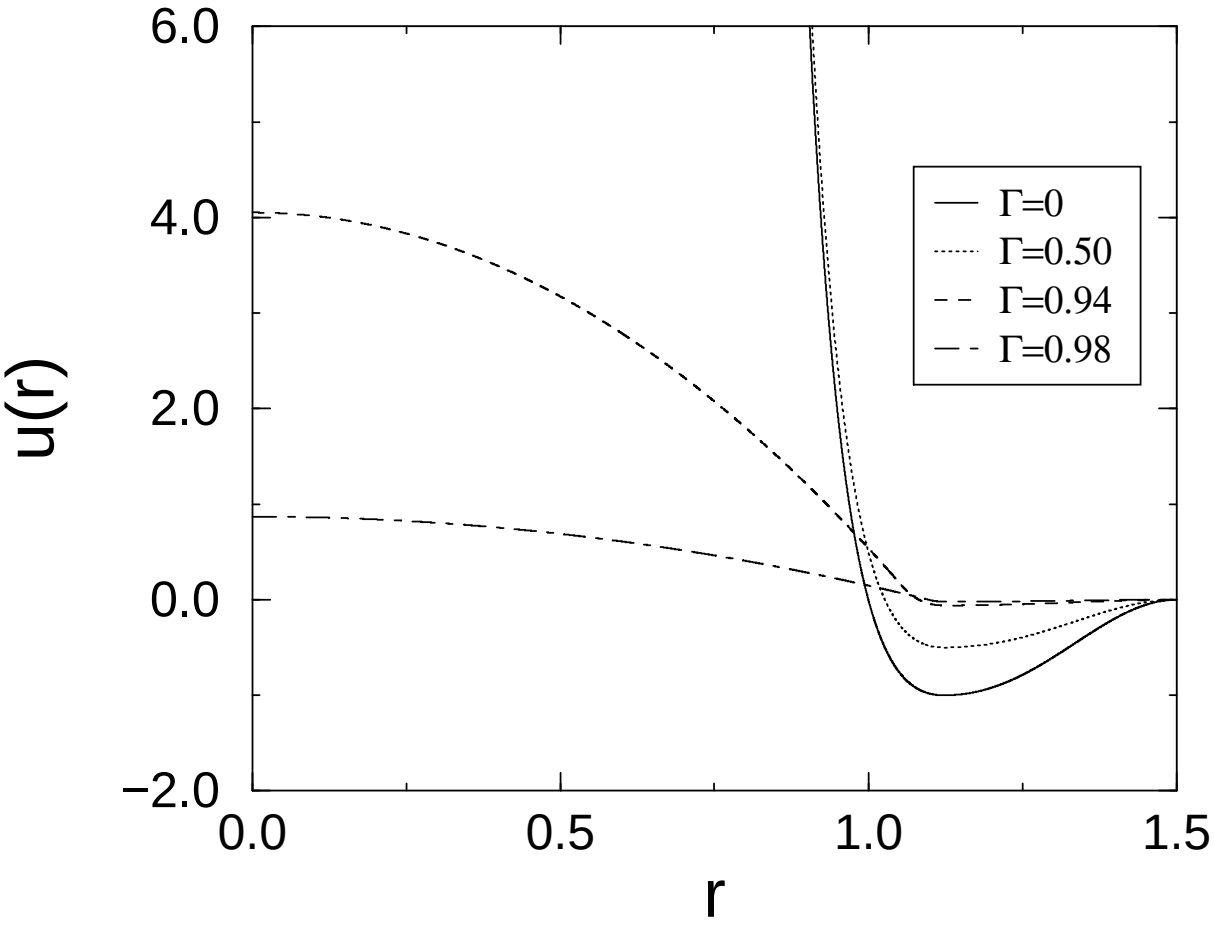

Figure 1 (Right)

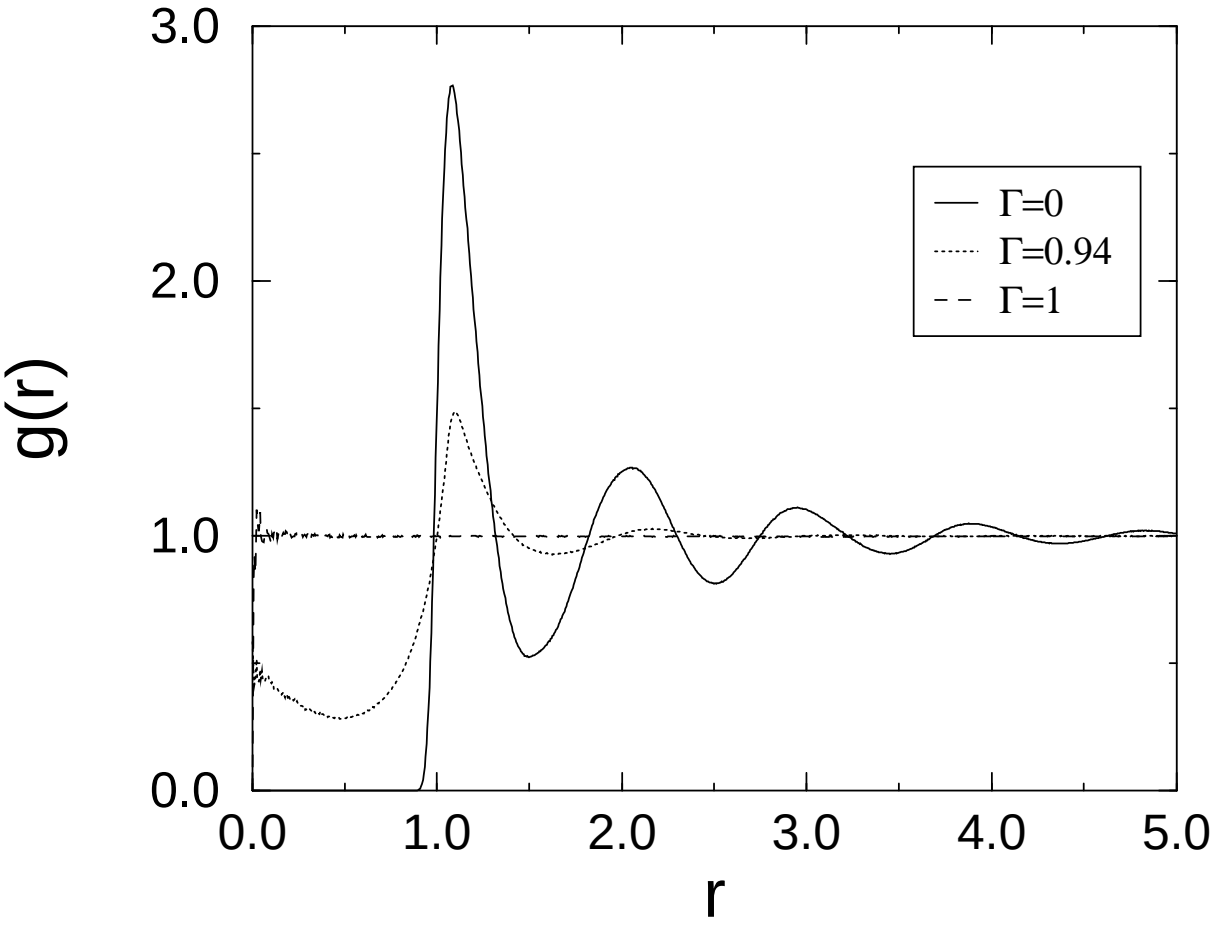

Figure 2

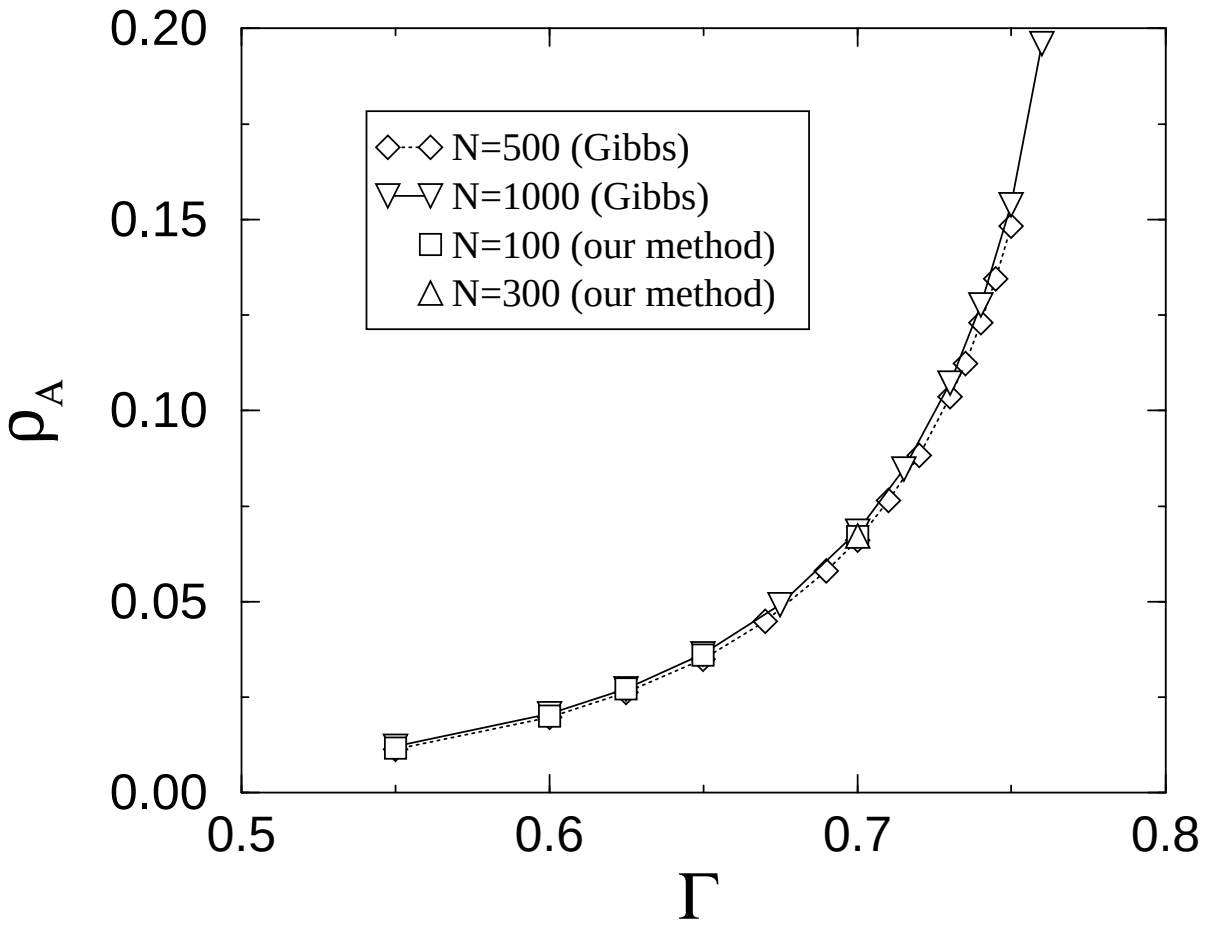
0.20
0.15
0.10
0.05
0.00
0.5
0.6
0.7
0.8
Γ
ρA
N=500 (Gibbs)
N=1000 (Gibbs)
N=100 (our method)
N=300 (our method)

Figure 3 (Left)

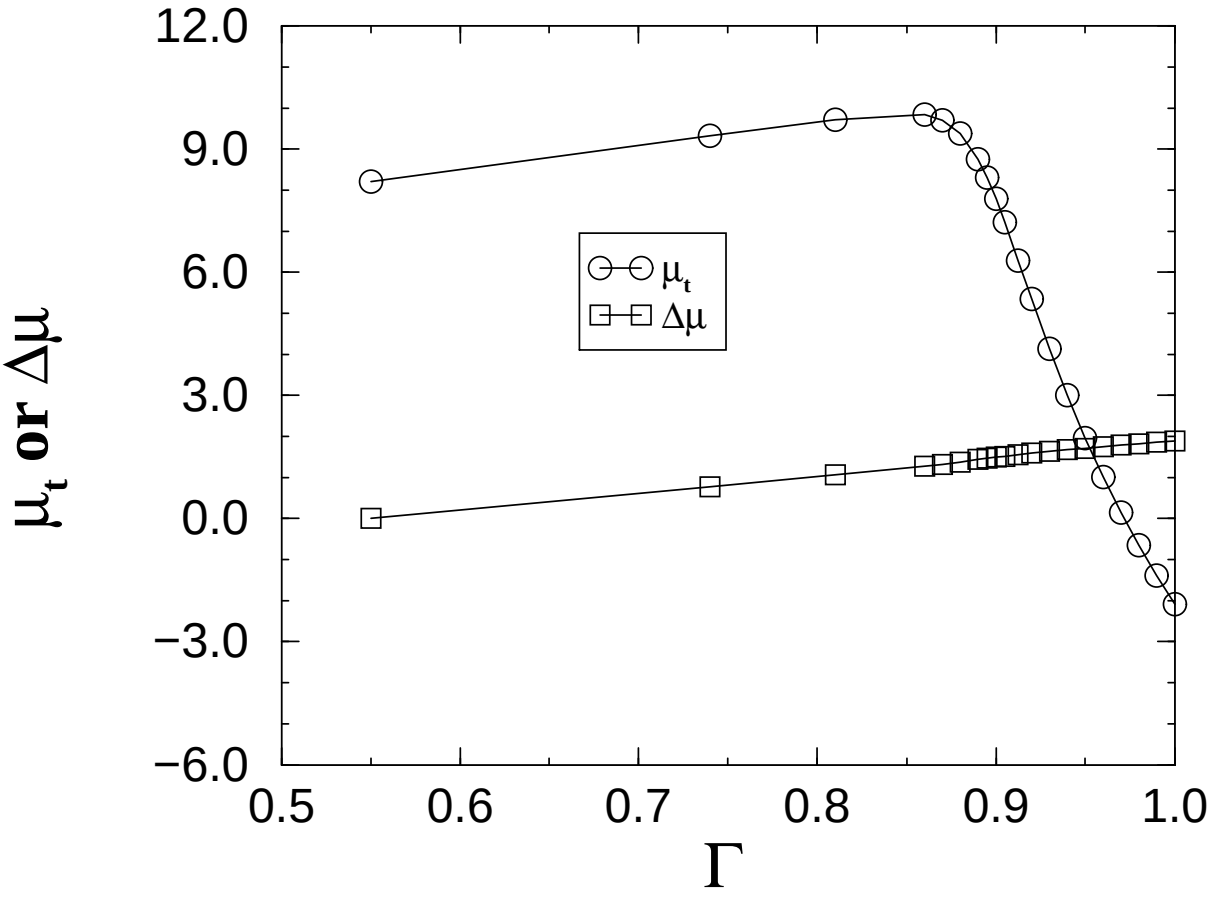

Figure 3 (Right)

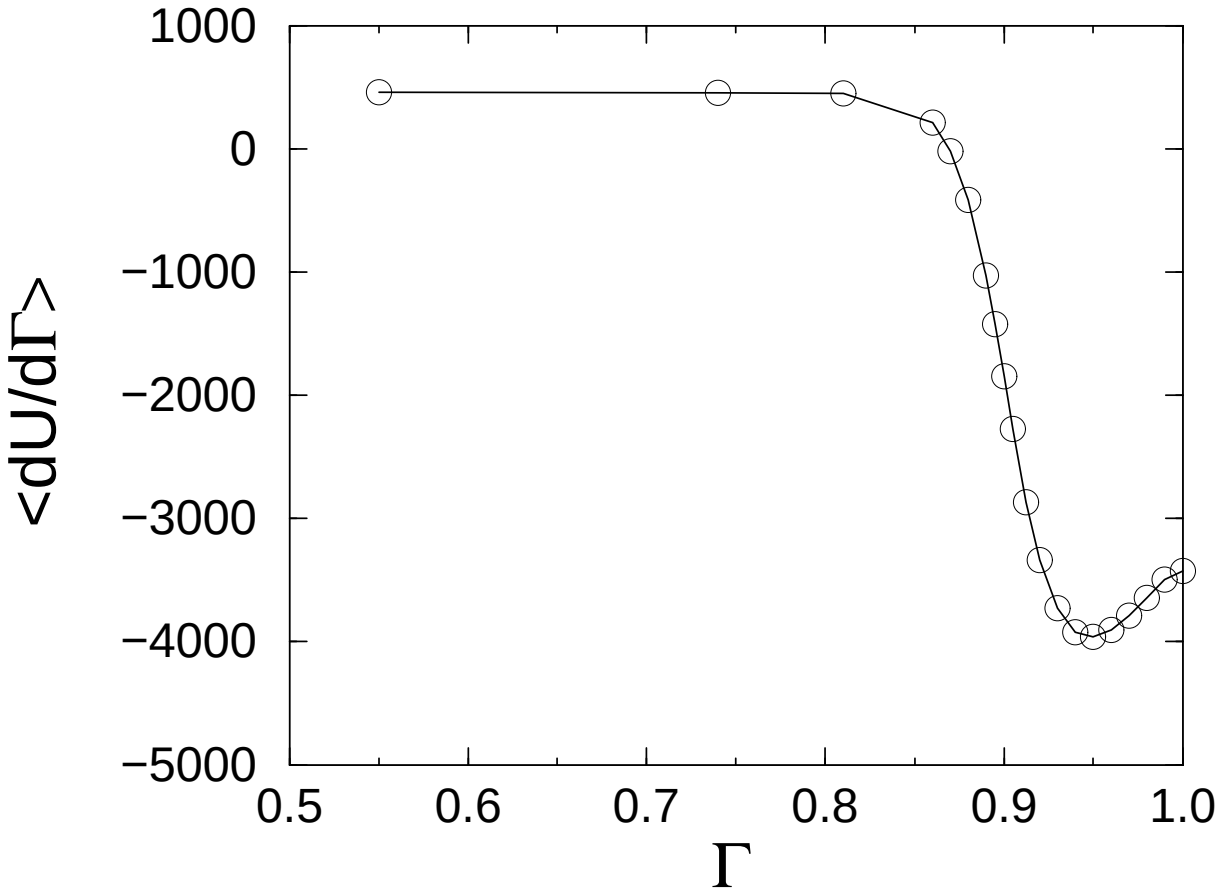

Figure 4

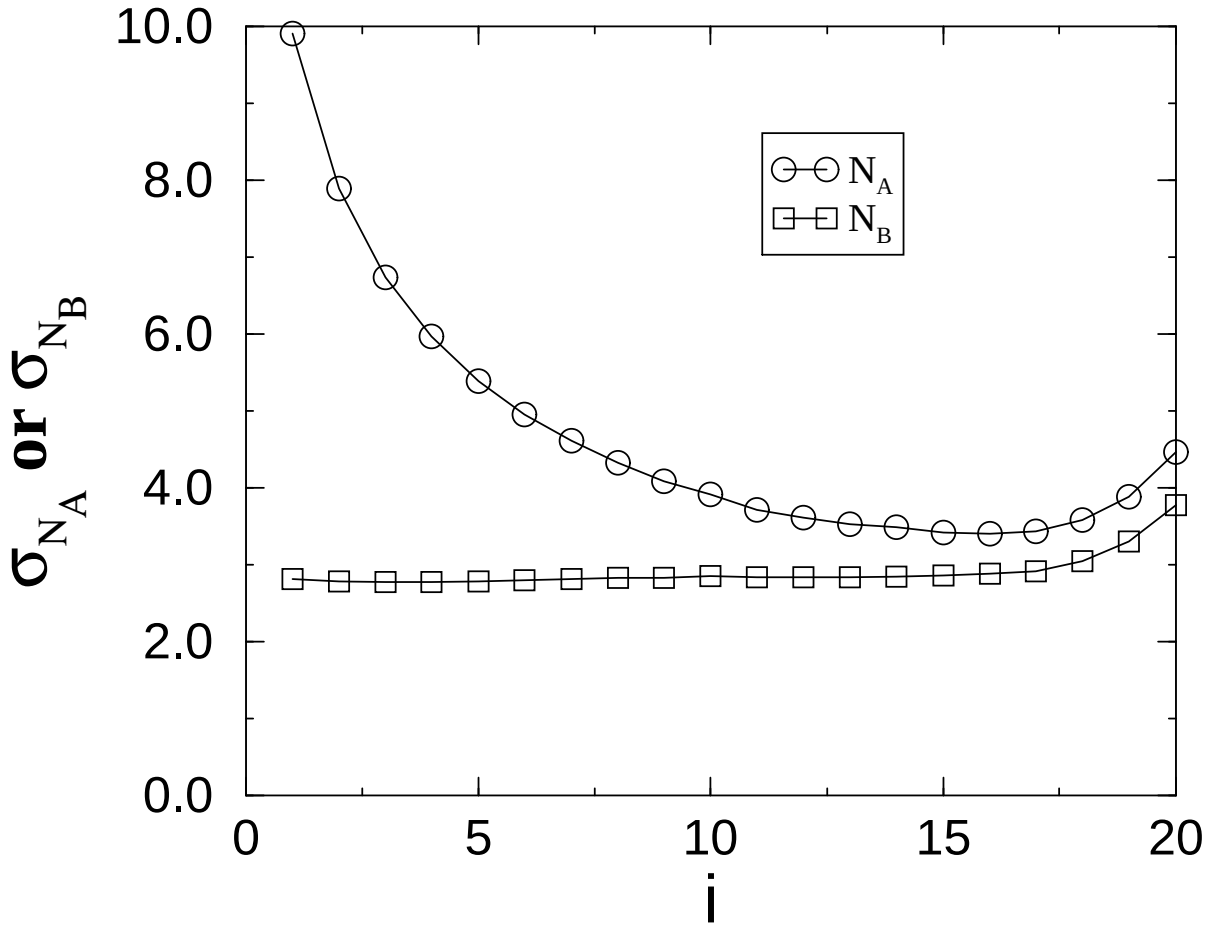

Figure 5 (Left)

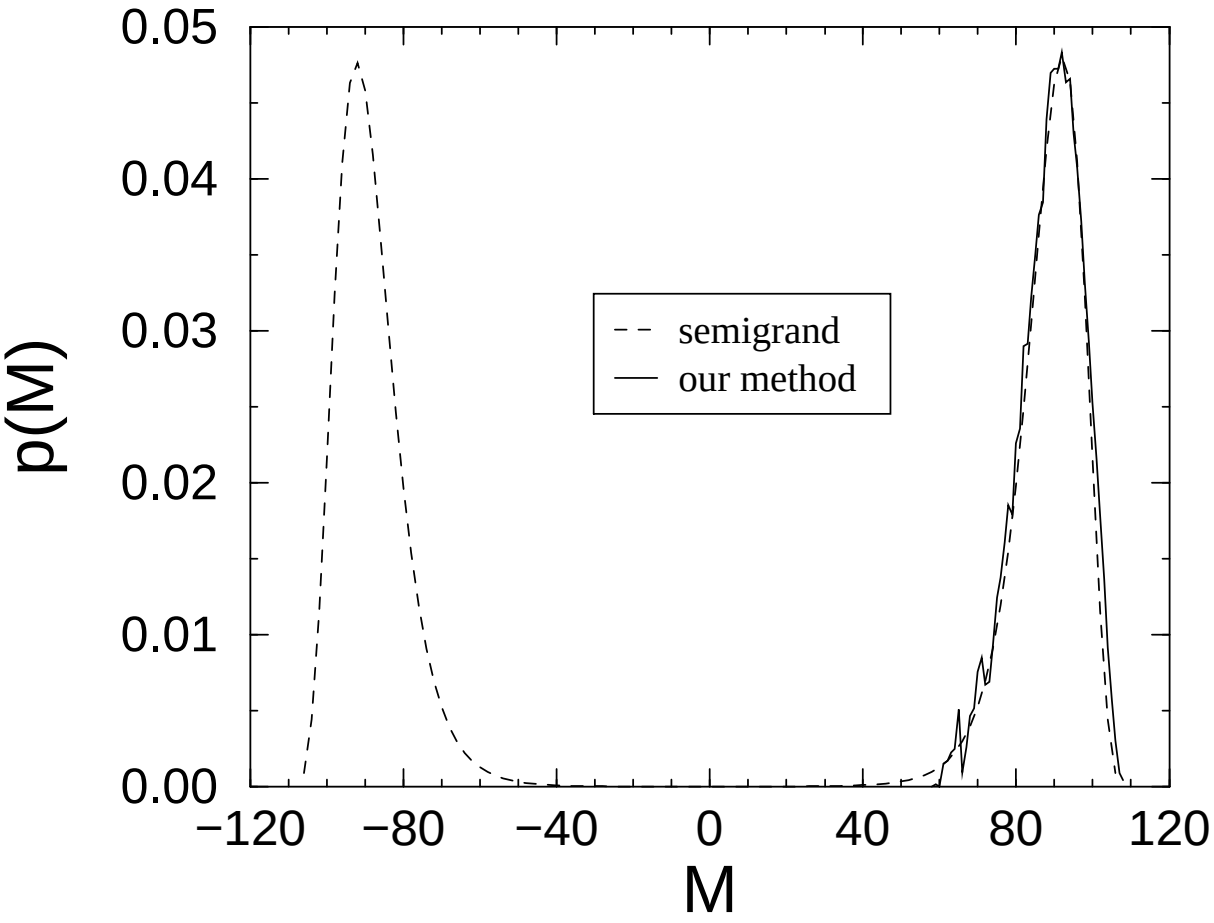

Figure 5 (Right)

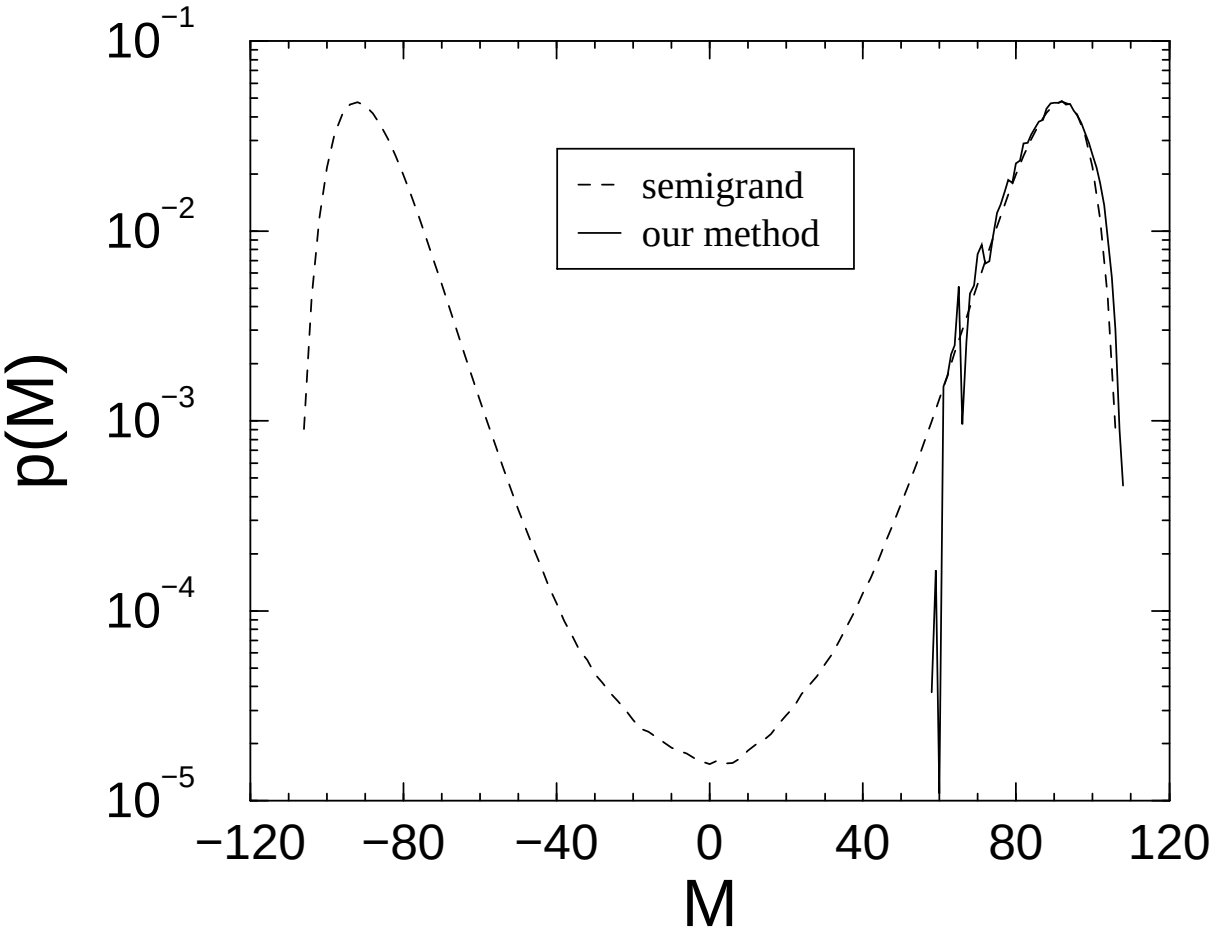

Figure 6

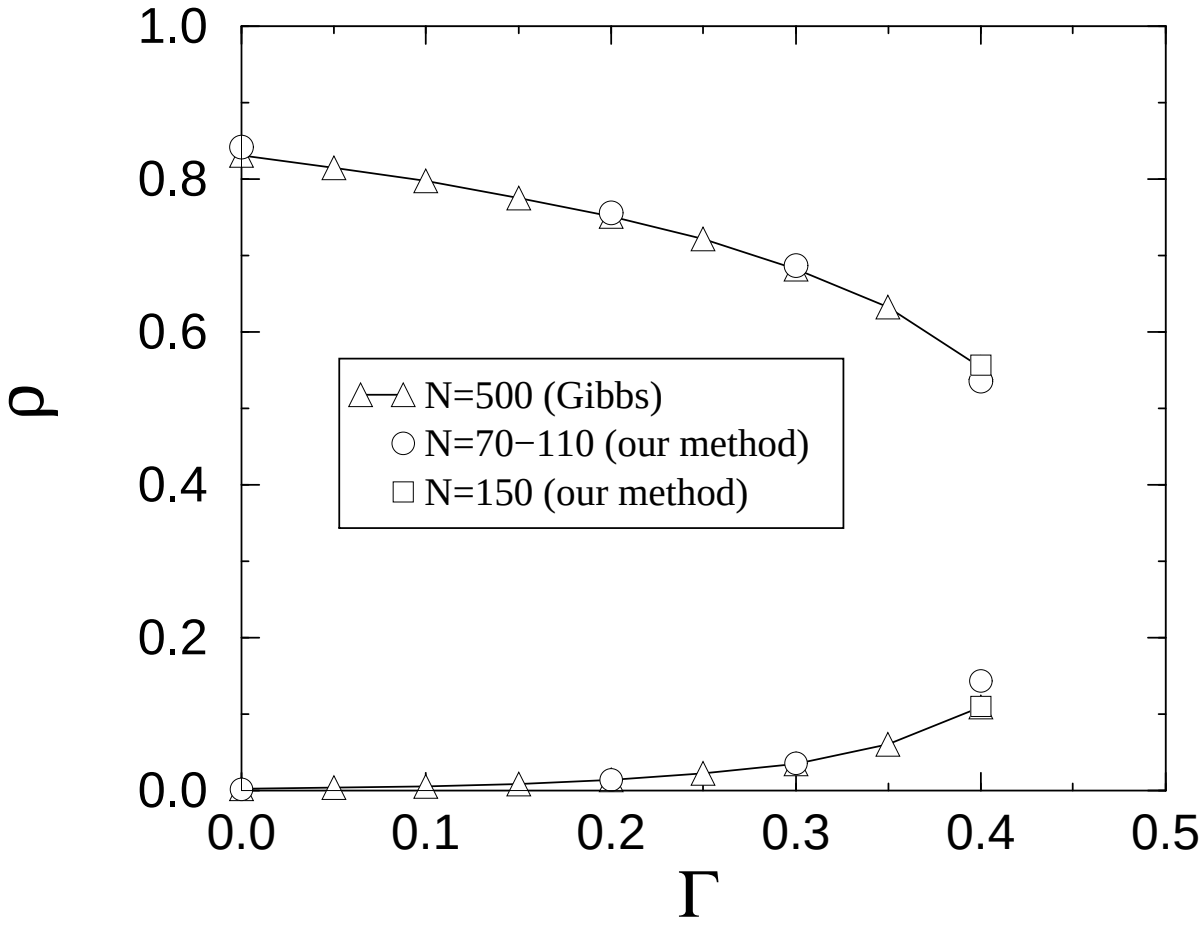
1.0
0.8
0.6
0.4
0.2
0.0
ρ
0.0
0.1
0.2
0.3
0.4
0.5
Γ
N=500 (Gibbs)
N=70−110 (our method)
N=150 (our method)

Figure 7 (Left)

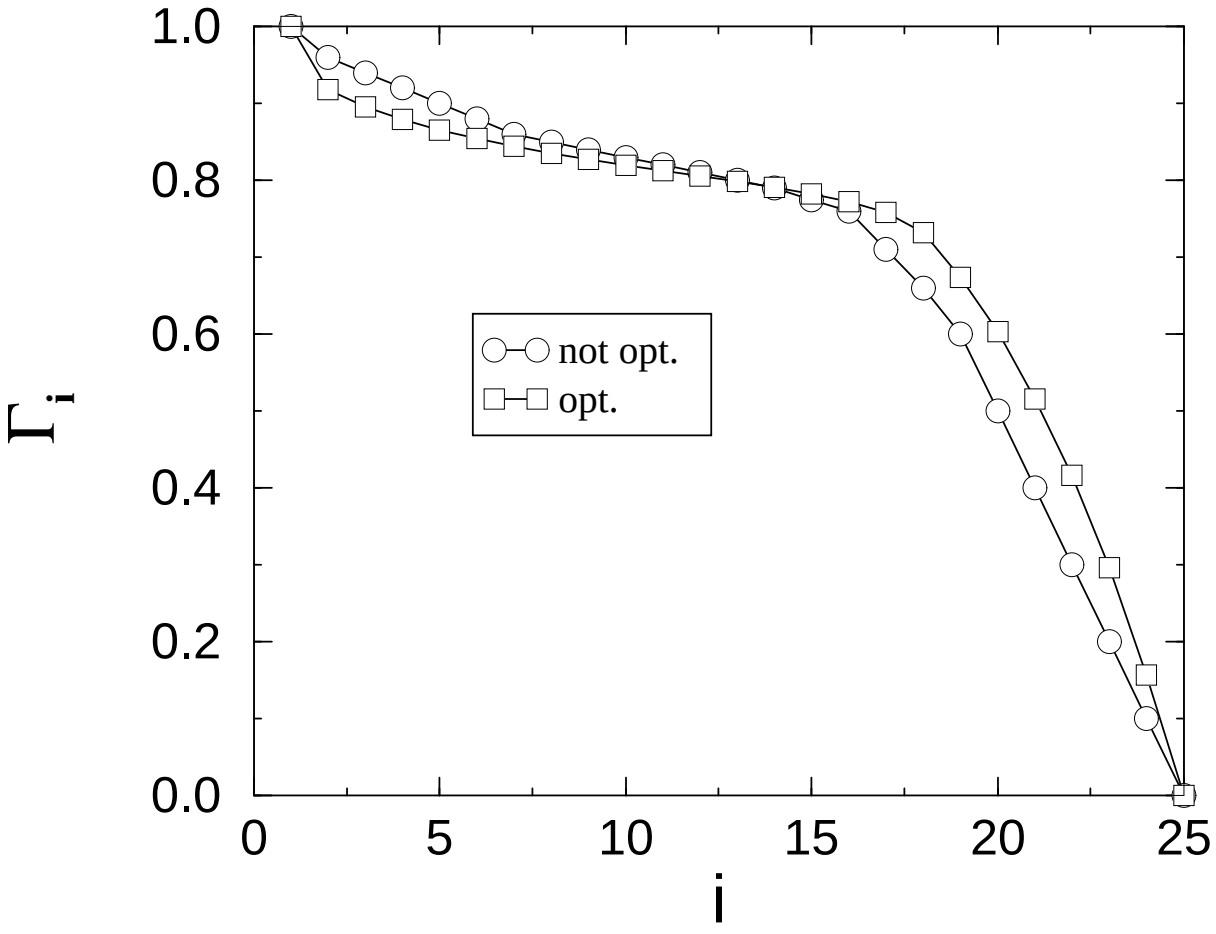

Figure 7 (Right)